EPJ Web of Conferences **259**, 11005 (2022) https://doi.org/10.1051/epjconf/202225911005
SQM 2021

Multi-strange hadron production in p+p interactions at $\sqrt{s_{NN}}$=17.3 GeV

Szymon Pulawski[1,*]
for the NA61/SHINE Collaboration

[1]Institute of Physics, University of Silesia, Katowice

Abstract. The production of multi-strange hadrons in proton-proton interactions is currently studied with the NA61/SHINE experiment at the SPS. These particles are reconstructed via their weak decay typologies, exploiting the tracking and particle identification capabilities of NA61/SHINE. New measurements of rapidity and transverse momentum spectra of Ξ^- and Ξ resonances and their antiparticles are shown. The results are compared to those observed in A+A collisions as well as to model predictions.

1 NA61/SHINE facility

The data used for the analysis were recorded at the CERN SPS accelerator complex with the NA61/SHINE fixed target large acceptance hadron detector [1]. The NA61/SHINE tracking system consists of 4 large volume time projection chambers (TPCs). Two of the TPCs (VTPC1 and VTPC2) are within superconducting dipole magnets. Downstream of the magnets, two larger TPCs (MTPC-R and MTPC-L) provide acceptance at high momenta. The fifth small TPC (GAP-TPC) is placed between VTPC1 and VTPC2 directly on the beamline. The interactions were measured in the H2 beamline in the North Experimental Hall with a secondary beam of 158 GeV/c protons impinging on a cylindrical Liquid Hydrogen Target (LHT) of 20 cm length and 2 cm diameter. This beam was produced by 400 GeV/c protons hitting a Be-target. The primary protons were extracted from the SPS in a slow extraction mode with a flat top lasting about 10 seconds. Protons and other positively charged particles produced in the Be-target constitute the secondary hadron beam. Two Cherenkov counters identified the protons, a CEDAR (either CEDAR-W or CEDAR-N) and a threshold counter (THC). A selection based on signals from the Cherenkov counters identified the protons with a purity of about 99% [2]. A set of scintillation counters selects individual beam particles. Their trajectories are precisely measured by three beam position detectors (BPD-1, BPD-2, BPD-3) [1].

2 Multi-strange measurements

The presented results cover doubly strange hyperon production in inelastic p+p interactions at 158 GeV/c corresponding to $\sqrt{s_{NN}}$=17.3 GeV. Results are corrected for losses due to limited geometrical detector acceptance and reconstruction efficiency, as well as for secondary interactions and branching ratios to unmeasured channels.

*e-mail: szymon.pulawski@us.edu.pl

A total of 33 million minimum bias $p + p$ at 158 GeV/c events were recorded in 2009, 2010, and 2011 and analysed. Interactions in the target are selected with the trigger system and offline selection criteria.

Multi-strange hyperons are identified by their decay typologies. The $\Xi(1530)^0$ is produced in the primary interaction and decays strongly into Ξ^- and π^+. Then the Ξ^- travels for some distance, after which it decays into a Λ and a π^-. Subsequently the Λ decays into a proton and a π^-. A schematic drawing of the $\Xi(1530)^0$ decay chain is shown in Fig. 1.

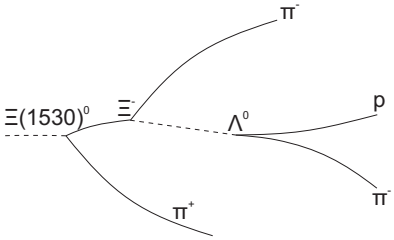

Figure 1. Schematic sketch of the $\Xi(1530)^0$ decay scheme.

2.1 Ξ production in inelastic $p + p$ collisions at 158 GeV/c

The p_T spectra in successive rapidity intervals of Ξ^- and $\overline{\Xi}^+$ measured in $p + p$ collisions at 158 GeV/c [3] are shown in Fig. 2 and scaled by appropriate factors for better visibility.

Rapidity distributions were then obtained by summing the measured transverse momentum spectra and extrapolating them into the unmeasured regions using the fitted functions. The resulting rapidity distributions are shown in Fig. 3.

The NA61/SHINE data on charged Ξ production in inelastic $p + p$ interactions are compared with predictions of the following microscopic models: Epos 1.99 [4], Urqmd 3.4 [5, 6], Ampt 1.26 [7–9], Smash 1.6 [10, 11] and Phsd [12, 13]. The model predictions are compared with the NA61/SHINE data in figs. 4. Epos 1.99 describes well the Ξ^- and $\overline{\Xi}^+$ rapidity spectra but fails on the shape of the transverse momentum distribution. The comparison of the Urqmd 3.4 calculations with the NA61/SHINE measurements reveals major discrepancies for the $\overline{\Xi}^+$ hyperons. The model output describes almost perfectly the rapidity and transverse momentum spectra of Ξ^- but strongly overestimates $\overline{\Xi}^+$ yields. Consequently also the ratio of $\overline{\Xi}^+$ to Ξ^- cannot be described by the Urqmd model, see Fig. 5(c). The Ampt, Smash and Phsd models fail in the description of both transverse momentum spectra and rapidity distributions. Ampt overestimates the Ξ^- and $\overline{\Xi}^+$ multiplicities while Smash underestimates them, both failing to describe the ratio. Phsd underestimates the Ξ^- yields and overestimates $\overline{\Xi}^+$. Obviously Phsd also fails to describe the ratio. Epos differs from the Urqmd, Ampt, Smash and Phsd models in its treatment of Pomeron-Pomeron interactions and of the valence quark remnants at the string ends.

2.2 Strangeness enhancement factors

The Ξ mean multiplicities measured by NA61/SHINE in inelastic $p + p$ interactions are used to calculate the enhancement factors of Ξs observed in centrality selected Pb+Pb, in semi-central C+C, and in Si+Si collisions as measured by NA49 [15] at the CERN SPS. The results

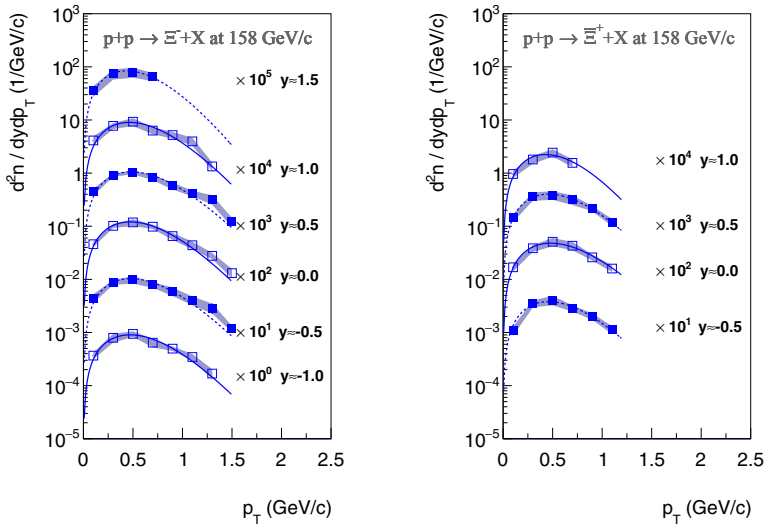

Figure 2. (Color online) Transverse momentum spectra in rapidity slices of Ξ^- (*left*) and $\overline{\Xi}^+$ (*right*) produced in inelastic $p+p$ interactions at 158 GeV/c. Rapidity values given in the legends correspond to the middle of the corresponding interval. Statistical uncertainties are smaller than the marker size, shaded bands show systematic uncertainties. Spectra are scaled by the given factors for better separation.

for mid-rapidity densities are shown in Fig. 6 (*left*) as a function of $\langle N_W \rangle$. The enhancement factor increases approximately linearly from 3.5 in C+C to 9 in central Pb+Pb collisions. This result is compared to data from the NA57 experiment at the SPS [16], the STAR experiment at the Relativistic Heavy Ion Collider (RHIC) [17] and the ALICE experiment at the Large Hadron Collider (LHC) [18]. The published enhancement factor reported by NA57 at the CERN SPS was computed using p+Be instead of inelastic $p + p$ interactions. Since strangeness production is already slightly enhanced in p+A collisions [19], this is not a proper reference. With the advent of the NA61/SHINE results on Ξ production in $p + p$ interactions a new baseline reference becomes available and it is used here for the recalculation of the enhancement observed in the NA57 p+Be and A+A data. The STAR Collaboration published results on multi-strange hyperon production in Au+Au collisions at $\sqrt{s_{NN}}$ from 7.7 to 39 GeV [20], however the corresponding data on $p + p$ and p+A interactions are missing. The agreement between the enhancement factors calculated using the NA49 and the NA57 A+A (p+Be) data is satisfactory. The STAR data show a slightly lower enhancement, but the enhancement observed by ALICE is significantly lower. Figure 6 (*right*) shows the rapidity densities dn/dy of $\overline{\Xi}^+$ at mid-rapidity per mean number of wounded nucleons divided by the corresponding values for inelastic $p+p$ collisions as a function of $\langle N_W \rangle$. Apart from a slightly flatter rise the overall picture remains unchanged.

2.3 $\Xi(1530)^0$ production in $p + p$ at 158 GeV/c

The $\Xi(1530)^0$ ($\overline{\Xi}(1530)^0$) yields are determined in 4 (4) rapidity and between 5 (3) and 6 (5) transverse momentum bins. The former is 0.5 units and the latter 0.3 GeV/c wide. The resulting (y, p_T) yields are presented as the function of p_T in Fig. 7. The p_T spectra in

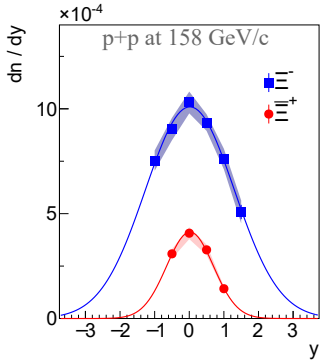

Figure 3. (Color online) Rapidity spectra of Ξ^- (blue squares) and $\overline{\Xi}^+$ (red circles) produced in inelastic $p + p$ interactions at 158 GeV/c. Statistical uncertainties are smaller than the marker size, shaded bands correspond to systematic uncertainties of the measurements. Curves depict Gaussian fits used to determine total mean multiplicities.

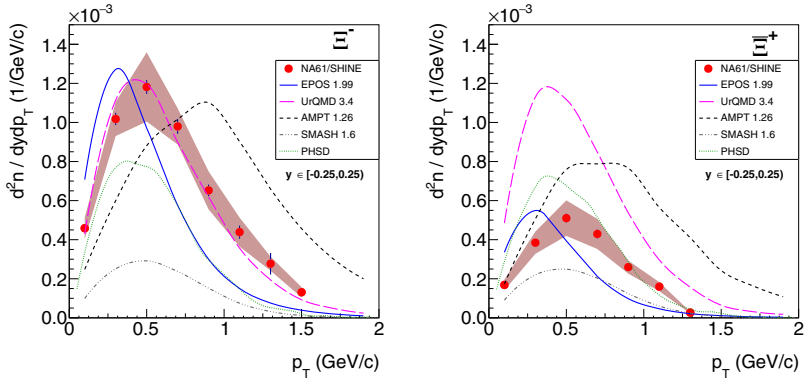

Figure 4. (Color online) Transverse momentum spectra at mid-rapidity of Ξ^- (*left*) and $\overline{\Xi}^+$ (*right*) produced in inelastic $p + p$ interactions at 158 GeV/c. Rapidity range is included in the legends. Shaded bands show systematic uncertainties. Urqmd 3.4 [5, 6], Epos 1.99 [4], Ampt 1.26 [7–9], Smash 1.6 [10, 11, 14] and Phsd [12, 13] predictions are shown as magenta, blue, black, gray and green lines, respectively.

successive rapidity intervals (Fig. 7) are scaled for better visibility. Statistical uncertainties are shown as error bars, and shaded bands correspond to systematic uncertainties.

The NA61/SHINE measurements of $\Xi(1530)^0$ and $\overline{\Xi}(1530)^0$ production are essential for understanding multi-strange particle production in elementary hadron interactions. The experimental results of NA61/SHINE are compared with predictions of the Epos 1.99 [4] and Urqmd 3.4 [5, 6] models in Figs. 8 and 9. Epos 1.99 describes well the $\Xi(1530)^0$ and $\overline{\Xi}(1530)^0$ transverse momentum and rapidity spectra. The comparison of the Urqmd 3.4 calculations with the NA61/SHINE measurements reveals significant discrepancies. The model strongly

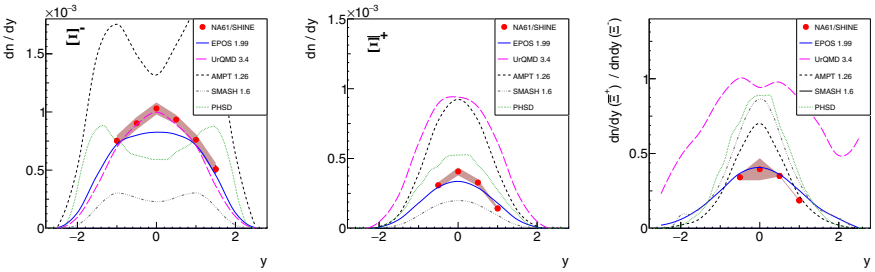

Figure 5. (Color online) Rapidity spectra of Ξ^- (*left*), $\overline{\Xi}^+$ (*middle*) and $\overline{\Xi}^+/\Xi^-$ ratio (*right*) measured in inelastic $p+p$ interactions at 158 GeV/*c*. Shaded bands show systematic uncertainties. UrQMD 3.4 [5, 6], EPOS 1.99 [4], AMPT 1.26 [7–9], SMASH 1.6 [10, 11, 14] and PHSD [12, 13] predictions are shown as magenta, blue, black, gray and green lines, respectively.

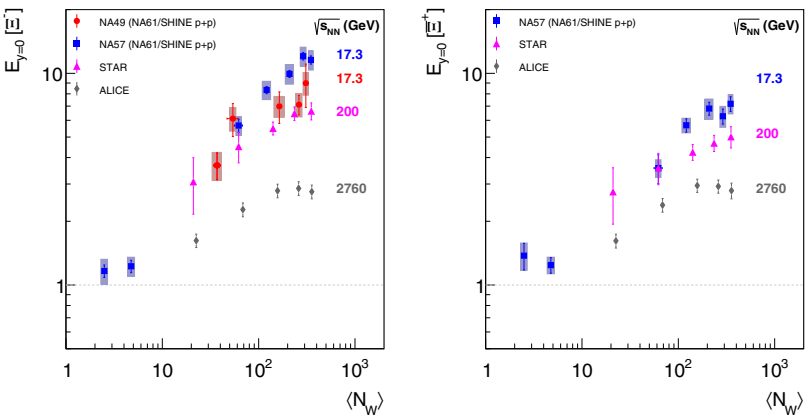

Figure 6. (Color online) The strangeness enhancement E at mid-rapidity as a function of average number of wounded nucleons $\langle N_W \rangle$ calculated as a ratio of rapidity density for Ξ^- production (*left*) and $\overline{\Xi}^+$ production (*right*) in nucleus-nucleus interactions per $\langle N_W \rangle$ divided by the corresponding value for $p+p$ interactions. Red circles – NA49 Pb+Pb at 158*A* GeV [15], blue squares - NA57 p+Be, p+Pb and Pb-Pb at the same center-of-mass energy $\sqrt{s_{NN}}$ = 17.3 GeV [16], magenta triangles - STAR Au+Au at $\sqrt{s_{NN}}$ = 200 GeV [17], gray diamonds - ALICE Pb+Pb at $\sqrt{s_{NN}}$ = 2.76 TeV [18]. The systematic errors are represented by shaded boxes.

overestimates $\Xi(1530)^0$ and $\overline{\Xi}(1530)^0$ yields. The ratio of $\overline{\Xi}(1530)^0$ to $\Xi(1530)^0$ cannot be described by the UrQMD model but is well reproduced by EPOS 1.99 (see Figs. 9 and 8).

3 HRG model in the CE formulation and $p+p$ data

The new measurements by NA61/SHINE of $\Xi(1530)^0$ and $\overline{\Xi}(1530)^0$ produced in inelastic $p+p$ interactions at 158 GeV/*c* as well as previously obtained results for π^+, π^-, K^+, K^-, p, $\overline{p}$, $K^*(892)^0$, Λ, $\phi(1020)$, Ξ^- and $\overline{\Xi}^+$ (see Refs. [2, 3, 21–25] were fitted by different variants of the Hadron Resonance Gas Model (HRG). The Canonical Ensemble with fixed $\gamma_s = 1$ and Canonical Ensemble with fitted strangeness saturation parameter γ_s configurations were

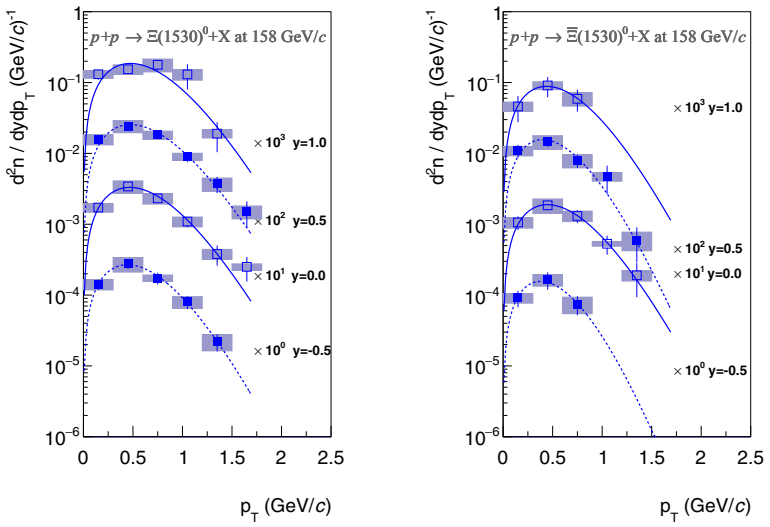

Figure 7. (Color online) Transverse momentum spectra in rapidity slices of $\Xi(1530)^0$ (*left*) and $\overline{\Xi}(1530)^0$ (*right*) produced in inelastic $p + p$ interactions at 158 GeV/*c*. Rapidity values given in the legends correspond to the middle of the corresponding interval. Statistical uncertainties are shown as vertical bars, and shaded bands show systematic uncertainties. Spectra are scaled for better visibility. Lines represent the fitted function.

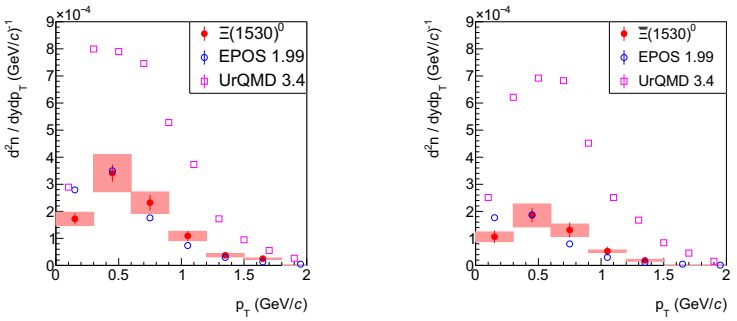

Figure 8. (Color online) Transverse momentum spectra at mid-rapidity of $\Xi(1530)^0$ (*left*) and $\overline{\Xi}(1530)^0$ (*right*) produced in inelastic $p + p$ interactions at 158 GeV/*c*. Shaded bands show systematic uncertainties. URQMD 3.4 [5, 6] and EPOS 1.99 [4] predictions are shown as magenta and blue markers, respectively.

used. Figure 10 compares the measured multiplicities of particles produced in inelastic $p + p$ interactions at 158 GeV/*c* with multiplicities of the same particles obtained from the HRG model in the CE formulation under two different model assumptions: $\gamma_s = 1$ and fitted γ_s. The software package THERMAL-FIST 1.3 [26] was used for this purpose. For the small $p + p$ system, the appropriate statistical system is the Canonical Ensemble, which has as parameters the Temperature T, the radius R of the system at chemical freezeout, and the strangeness

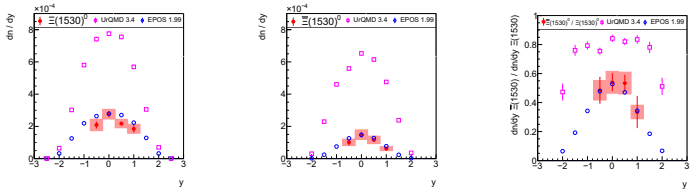

Figure 9. (Color online) Rapidity spectra of $\Xi(1530)^0$ (*left*), $\overline{\Xi}(1530)^0$ (*middle*) and $\overline{\Xi}(1530)^0/\Xi(1530)^0$ ratio (*right*) measured in inelastic $p + p$ interactions at 158 GeV/c. Shaded bands show systematic uncertainties. URQMD 3.4 [5, 6] and EPOS 1.99 [4] predictions are shown as magenta and blue points, respectively.

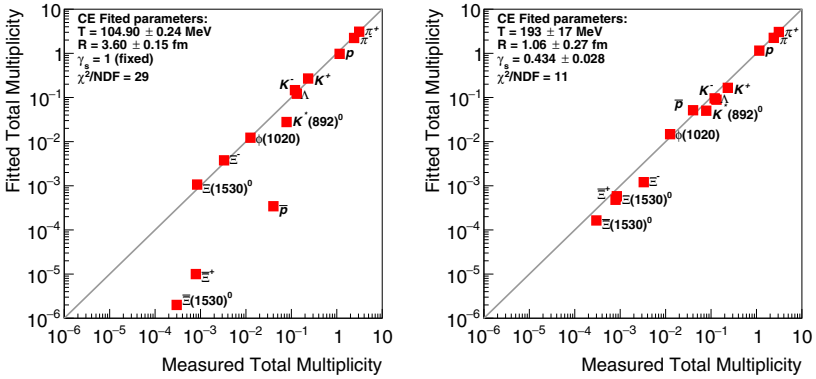

Figure 10. (Color online) Mean multiplicities of π^+, π^-, K^+, K^-, p, $\overline{p}$, $K^*(892)^0$, Λ, $\phi(1020)$, Ξ^-, $\overline{\Xi}^+$, $\Xi(1530)^0$ and $\overline{\Xi}(1530)^0$ produced in $p + p$ interactions at 158 GeV/c [2, 3, 21–25] measured by NA61/SHINE are compared with mean multiplicities obtained from the HRG model based on the Canonical Ensemble with fixed $\gamma_s = 1$ (*i*) and fitted γ_s (*ii*). Uncertainties of the measurement are smaller than the symbol size.

suppression factor γ_s. The results plotted in Fig. 10 show significant discrepancies for the fitted parameters T and R between the fits with $\gamma_s = 1$ and free γ_s. Moreover, the fit with fixed γ_s shows unacceptably large χ^2/NDF = 29. This demonstrates that the statistical model fails when fixing γ_s to one. The fit with free γ_s finds $\gamma_s = 0.434 \pm 0.028$ and reproduces the measurements rather well. Thus the statistical model indicates a strong suppression of strange particle production in $p + p$ collisions at CERN SPS energies.

References

[1] N. Abgrall et al. (NA61/SHINE), JINST **9**, P06005 (2014), 1401.4699
[2] N. Abgrall et al. (NA61/SHINE), Eur.Phys.J. **C74**, 2794 (2014), 1310.2417
[3] A. Aduszkiewicz et al. (NA61/SHINE), Eur. Phys. J. C **80**, 833 (2020), 2006.02062
[4] K. Werner, Nucl. Phys. Proc. Suppl. **175-176**, 81 (2008)
[5] S. Bass et al., Prog.Part.Nucl.Phys. **41**, 255 (1998), nucl-th/9803035
[6] M. Bleicher et al., J.Phys. **G25**, 1859 (1999), hep-ph/9909407
[7] Z.W. Lin, C.M. Ko, B.A. Li, B. Zhang, S. Pal, Phys. Rev. C **72**, 064901 (2005)

[8] Z.W. Lin, Phys. Rev. C **90**, 014904 (2014)
[9] B. Zhang, C.M. Ko, B.A. Li, Z. Lin, Phys. Rev. C **61**, 067901 (2000)
[10] J. Mohs, S. Ryu, H. Elfner, J. Phys. G **47**, 065101 (2020), 1909.05586
[11] J. Weil et al., Phys. Rev. C **94**, 054905 (2016), 1606.06642
[12] W. Cassing, E. Bratkovskaya, Nucl. Phys. A **831**, 215 (2009), 0907.5331
[13] W. Cassing, E. Bratkovskaya, Phys. Rev. C **78**, 034919 (2008), 0808.0022
[14] D. Oliinychenko, V. Steinberg, J. Weil, M. Kretz, H.E. (Petersen), J. Staudenmaier, S. Ryu, A. Schäfer, J. Rothermel, J. Mohs et al., *smash-transport/smash: Smash-1.6* (2019)
[15] T. Anticic et al. (NA49), Phys. Rev. C **80**, 034906 (2009), 0906.0469
[16] F. Antinori et al. (NA57), J. Phys. G **32**, 427 (2006), nucl-ex/0601021
[17] B. Abelev et al. (STAR), Phys. Rev. C **77**, 044908 (2008), 0705.2511
[18] B.B. Abelev et al. (ALICE), Phys. Lett. B **728**, 216 (2014), [Erratum: Phys.Lett.B 734, 409–410 (2014)], 1307.5543
[19] T. Susa (NA49), Nucl. Phys. A **698**, 491 (2002)
[20] J. Adam et al. (STAR) (2019), 1906.03732
[21] A. Aduszkiewicz et al. (NA61/SHINE), Eur. Phys. J. **C77**, 671 (2017), 1705.02467
[22] A. Aduszkiewicz et al. (NA61/SHINE), Phys. Rev. C **102**, 011901 (2020), 1912.10871
[23] A. Aduszkiewicz et al. (NA61/SHINE), Eur. Phys. J. C **80**, 460 (2020), 2001.05370
[24] A. Aduszkiewicz et al. (NA61/SHINE), Eur. Phys. J. C **80**, 199 (2020), 1908.04601
[25] A. Aduszkiewicz et al. (NA61/SHINE), Eur. Phys. J. **C76**, 198 (2016), 1510.03720
[26] V. Vovchenko, H. Stoecker, Comput. Phys. Commun. **244**, 295 (2019), 1901.05249